Mon. Not. R. Astron. Soc. **000**, 1–12 (2008) Printed 4 September 2008 (MN LaTeX style file v2.2)

arXiv:0809.0891v1 [astro-ph] 4 Sep 2008

Spatially-Resolved Medium Resolution Spectroscopy of an Interacting E+A (post-starburst) System with the Subaru telescope*

Tomotsugu Goto[1,2] † ‡§ , Masafumi Yagi[2], and Chisato Yamauchi[3]
[1] *Institute for Astronomy, University of Hawaii 2680 Woodlawn Drive, Honolulu, HI, 96822, USA*
[2]*National Astronomical Observatory, 2-21-1 Osawa, Mitaka, Tokyo 181-8588,Japan*
[3] *Institute of Space and Astronautical Science, Japan Aerospace Exploration Agency, 3-1-1 Yoshinodai, Sagamihara, Kanagawa 229-8510, Japan*

4 September 2008; in original form 2008 April 28

ABSTRACT

We have performed a spatially-resolved medium resolution long-slit spectroscopy of a nearby E+A (post-starburst) galaxy system, SDSSJ161330.18+510335.5, with the FOCAS spectrograph mounted on the Subaru telescope. This E+A galaxy has an obvious companion galaxy 14kpc in front with the velocity difference of 61.8 km/s. Both galaxies have obviously disturbed morphology. Thus, this E+A system provides us with a perfect opportunity to investigate the relation between the post-starburst phenomena and galaxy-galaxy interaction.

We have found that Hδ equivalent width (EW) of the E+A galaxy is greater than 7Å galaxy wide (8.5 kpc) with no significant spatial variation. The E+A galaxy have a weak [OIII] emission (EW$\sim$1Å) by $\sim$2.6 kpc offset from the peak of the Balmer absorption lines. We detected a rotational velocity in the companion galaxy of $>$175km/s. The progenitor of the companion may have been a rotationally-supported, but yet passive S0 galaxy. We did not detect significant rotation on the E+A galaxy. Metallicity estimate based on the $r-H$ colour suggests $Z=0.008$ and 0.02, for the E+A and the companion galaxies, respectively. Assuming these metallicity estimates, the age of the E+A galaxy after quenching the star formation is estimated to be 100-500Myr, with its centre having slightly younger stellar population. The companion galaxy is estimated to have older stellar population of $>$2 gigayear of age with no significant spatial variation.

These findings are inconsistent with a simple picture where the dynamical interaction creates infall of the gas reservoir that causes the central starburst/post-starburst. Instead, our results present an important example where the galaxy-galaxy interaction can trigger a galaxy-wide post-starburst phenomena.

Key words: galaxies: evolution, galaxies:interactions, galaxies:starburst, galaxies:peculiar, galaxies:formation

1 INTRODUCTION

It has long been known that galaxies have varieties of morphology; Edwin Hubble was the first to classify galaxies into the so-called Hubble tuning fork, which mainly consists of elliptical, lenticular, spiral and barred spirals (Hubble 1926). Because of similarity and gradual change of galaxy properties along the Hubble's tuning fork, people speculated this might be an evolutionary sequence, and extensively studied the galaxy evolutionary sequence since the dawn of the extragalactic astronomy (e.g., Roberts & Haynes 1994). However, it is still not very well understood what physical mechanism drives the galaxy evolution, creating the diverse galaxy properties such as in the Hubble tuning fork. As a galaxy in a transition phase, one of the key populations in elucidating this galaxy evolution is so-called E+A galaxies.

Galaxies with strong Balmer absorption lines without any emission in [OII] nor Hα are called E+A galaxies. The existence of strong Balmer absorption lines shows that E+A galaxies have experienced starburst recently (within a gigayear; Goto 2004). However, these galaxies do not show any sign of

---

* Based on data collected at Subaru Telescope, which is operated by the National Astronomical Observatory of Japan.
† E-mail:tomo@ifa.hawaii.edu
‡ JSPS SPD Fellow
§ Visiting Astronomer, Kitt Peak National Observatory, National Optical Astronomy Observatory, which is operated by the Association of Universities for Research in Astronomy (AURA) under cooperative agreement with the National Science Foundation.

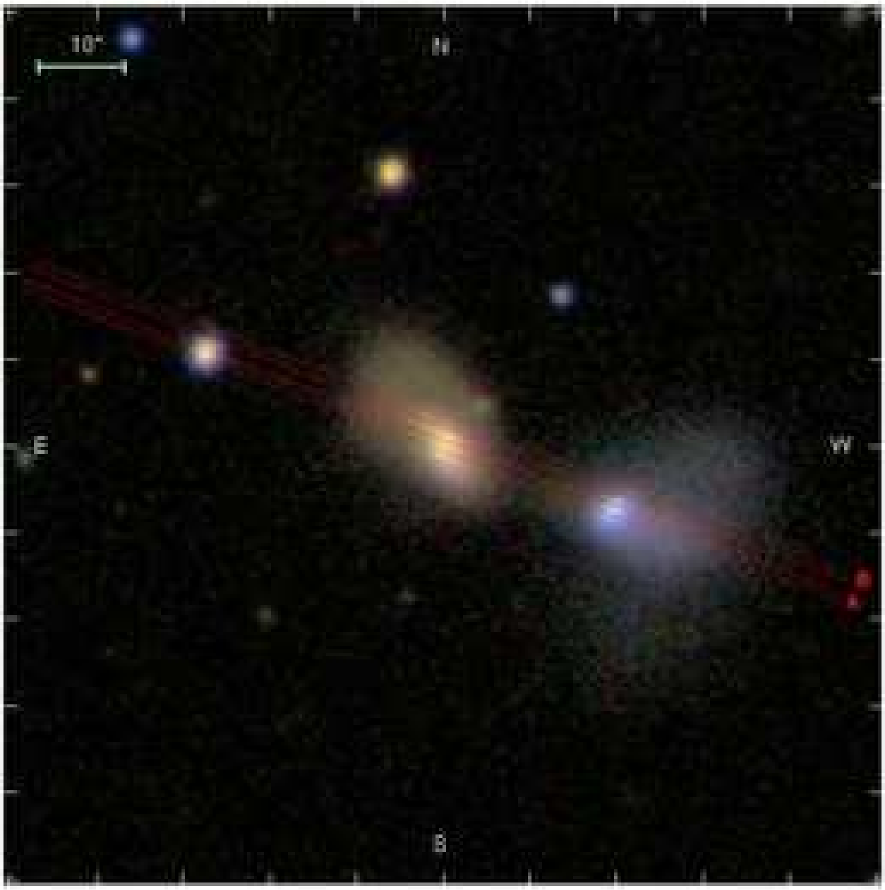

Figure 1. The SDSS g, r, i-composite image of the J1613+5103. The long-slit positions are overlayed. The E+A galaxy is to the right (west), with bluer colour. The companion galaxy is to the left (east).

on-going star formation as non-detection in the [OII] emission line indicates. Therefore, E+A galaxies have been interpreted as post-starburst galaxies, that is, a galaxy which truncated starburst suddenly (Dressler & Gunn 1983, 1992; Couch & Sharples 1987; MacLaren, Ellis, & Couch 1988; Newberry, Boroson, & Kirshner 1990; Fabricant, McClintock, & Bautz 1991; Abraham et al. 1996). Recent study found that E+A galaxies have α-element excess (Goto 2007a), which also supported the post-starburst interpretation of E+A galaxies. However, the reason why they started starburst, and why they abruptly stopped starburst remains one of the mysteries in the galaxy evolution. Since a post-starburst is an important stage of the overall galaxy evolution in the Universe, it is important to investigate the physical origin of the E+A galaxies.

At first, E+A galaxies are found in cluster regions, especially at higher redshift (Sharples et al. 1985; Lavery & Henry 1986; Couch & Sharples 1987; Broadhurst, Ellis, & Shanks 1988; Fabricant, McClintock, & Bautz 1991; Belloni et al. 1995; Barger et al. 1996; Fisher et al. 1998; Morris et al. 1998; Couch et al. 1998; Dressler et al. 1999; Poggianti et al. 1999; Tran et al. 2003; Dressler et al. 2004; Tran et al. 2004). Therefore a cluster specific phenomenon such as the ram-pressure stripping was thought to be responsible for the violent star formation history of E+A galaxies (Spitzer & Baade 1951; Gunn & Gott 1972; Farouki & Shapiro 1980; Kent 1981; Dressler & Gunn 1983; Abadi, Moore, & Bower 1999; Fujita et al. 1999; Quilis, Moore, & Bower 2000; Fujita, Takizawa, & Sarazin 2003; Bekki & Couch 2003; Fujita & Goto 2004).

However, Blake et al. (2004) found that low redshift E+A galaxies are located predominantly in the field environment, suggesting that a physical mechanism that works in the field region is at least partly responsible for these E+A galaxies. Recently, Goto (2005) has shown that E+A galaxies have more close companion galaxies than average galaxies, providing a statistical evidence that the dynamical merger/interaction could be the physical origin of field E+A galaxies. Dynamically disturbed morphologies of E+A galaxies also support this scenario (Liu et al. 2007; Yamauchi & Goto 2005).

To understand the origin of E+As is cluster-related or merger-driven (or both), independent evidence on the origin of E+A galaxies has been waited. Previous work mentioned above has been focused on the investigation of the global/external properties of E+A galaxies, such as the environment of E+A galaxies (Goto 2005), and the integrated spectra of the E+A galaxies (Dressler et al. 2004). However, if the physical origin of E+A galaxies is merger/interaction or gas-stripping, these mechanisms should leave traces to the spatial distribution of stellar-populations within each E+A galaxy. For example, a centrally-concentrated post-starburst region is expected to be found in case of the merger/interaction origin (e.g., Barnes & Hernquist 1992). In contrast, the gas-stripping would create a more uniform, galaxy-wide post-starburst region. Thus, the spatial-distribution of the post-

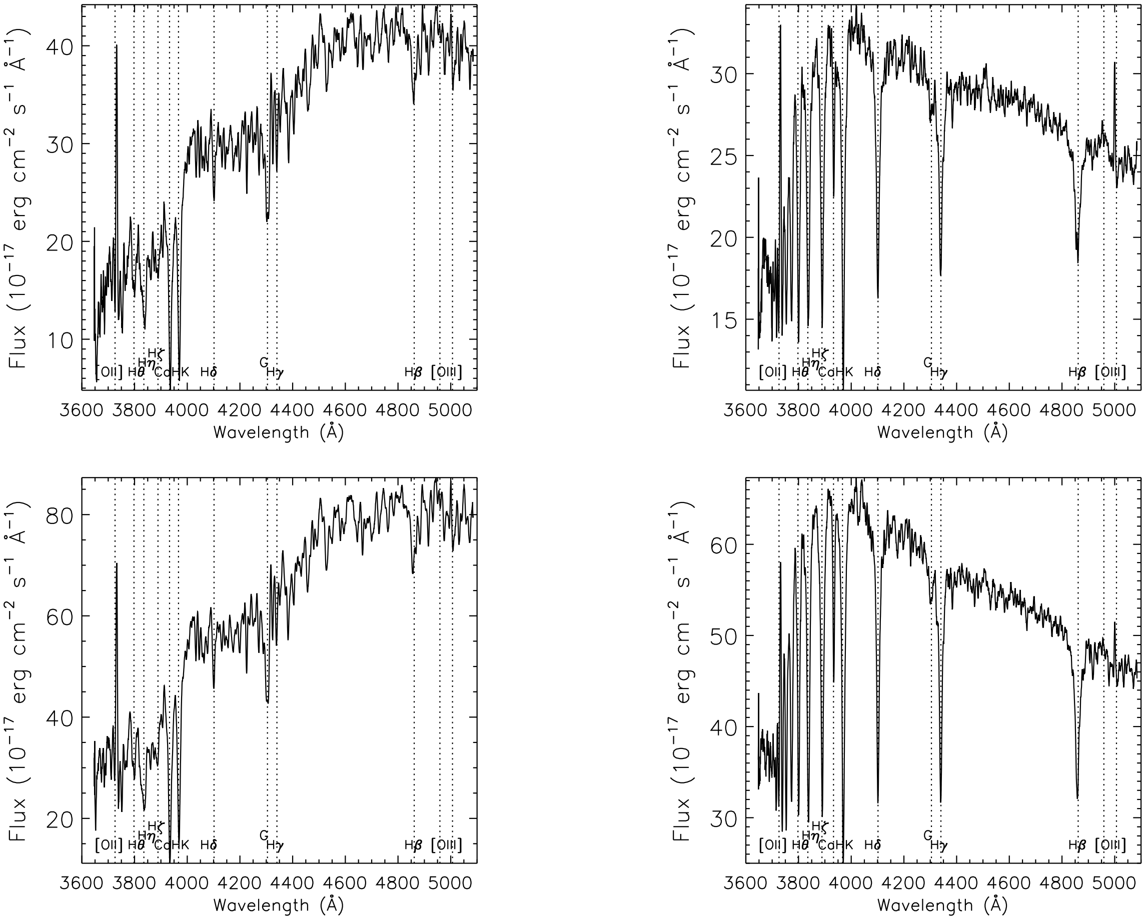

Figure 2. Spectra of the entire galaxy. Right panels are for the E+A galaxy. Left panels are for the companion galaxy. Bottom panels are from the core. Top panels are through the slit shifted by 2” to the north. The spectra are shifted to the rest-frame and smoothed using a 5-pixel box.

starburst region inside the E+A galaxy contains important and independent clues on the physical origin of E+A galaxies (e.g., Pracy et al. 2005; Swinbank et al. 2005). In this series of papers (Yagi & Goto 2006; Yagi, Goto, & Hattori 2006; Goto et al. 2008), we try to obtain such independent hints on the origin of E+A galaxies by revealing internal structure of E+A galaxies. In this paper, we focus on a spatially-resolved long-slit scan spectroscopy of a nearby E+A system J1613+5103. This E+A galaxy previously studied by Yagi, Goto, & Hattori (2006) has an obvious companion galaxy in front (Fig.1), and thus, provides us with a perfect opportunity to reveal the relation between the post-starburst phenomena and galaxy-galaxy interaction. Color gradient of the E+A galaxy is studied in detail by Yamauchi & Goto (2005). Compared to our own previous work (Yagi & Goto 2006; Yagi, Goto, & Hattori 2006; Goto et al. 2008), this time we obtained E+A spectra with higher resolution and better signal-to-noise taking advantage of the Subaru telescope.

Unless otherwise stated, we adopt the WMAP cosmology: $(h, \Omega_m, \Omega_L) = (0.7, 0.3, 0.7)$ (Komatsu et al. 2008).

2 SAMPLE SELECTION

We selected our target E+A galaxy, SDSSJ161330.18+510335.5, from Goto (2005, 2007b), which presented a catalog of 564 E+A galaxies based on the ∼670,000 galaxy spectra of the Sloan Digital Sky Survey (Adelman-McCarthy et al. 2006).

The galaxy has extremely strong Balmer absorption lines with the Hδ equivalent width (EW) of 7.37Å[1], without significant emission in [OII] nor Hα within the three arcsec diameter of the SDSS fiber spectrograph. These are representative characters of an E+A galaxy and indicate that this galaxy is in the post-starburst phase.

The E+A galaxy has an apparent companion galaxy, SDSSJ161332.23+510342.9, in front. Note that the companion galaxy is perhaps as massive as the E+A galaxy (see Section4.3), even though we call it a “companion”. Previously, Yagi, Goto, & Hattori (2006) confirmed that the companion galaxy is at the same redshift, i.e., these two galaxies are dynamically-interacting. Along with the large apparent size of ∼20 arcsec on the sky, this E+A system is a perfect target for spatially-resolved spectroscopy.

We present the basic properties of the E+A and companion galaxies in table 1, where measured quantities such as positions, redshift, magnitudes in g and r, and Petrosian radius are taken from the SDSS catalog. Magnitudes are de-reddened (for the Galactic extinction) Petrosian AB-magnitude in g and r-band.

---

[1] Absorption lines have a positive sign throughout this paper.

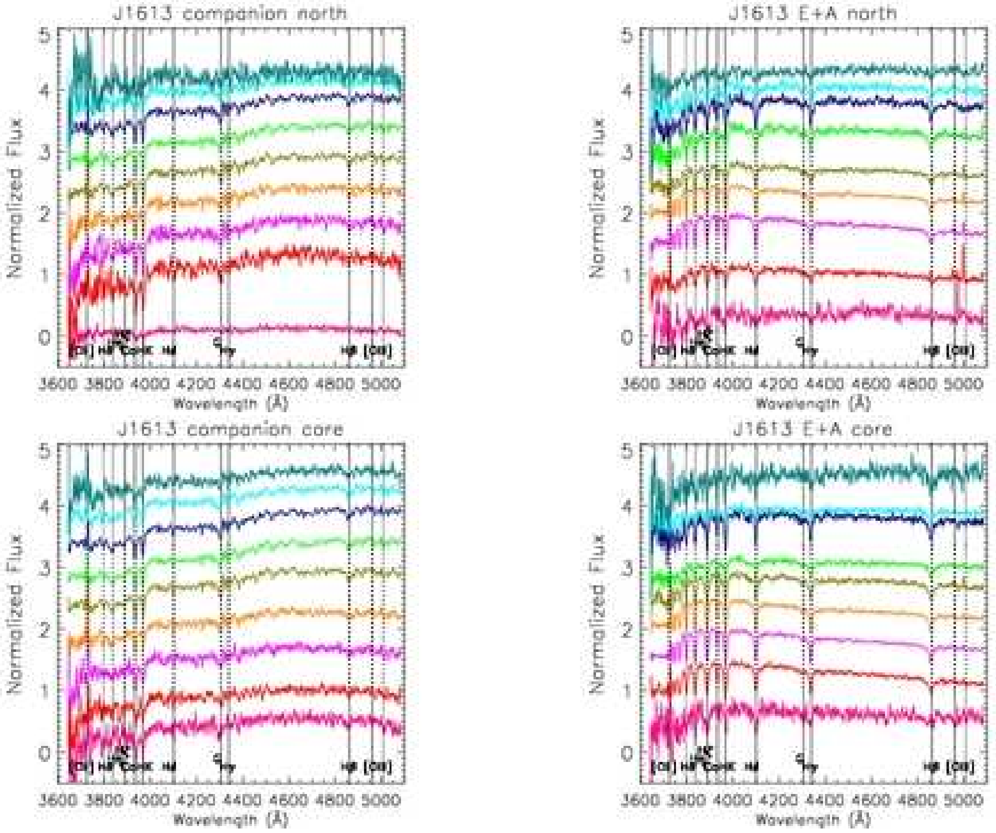

Figure 3. Spectra in each aperture. Right panels are for the E+A galaxy. Left panels are for the companion galaxy. Bottom panels are from the core. Top panels are shifted by 2” to the north. Each spectrum is spatially-divided into 9 equally-spaced bins. In each panel, these 9 spectra are normalized by the peak flux and aligned in the vertical direction (thus, the flux scale is arbitrary). The spectra are shifted to the rest-frame and smoothed using a 5-pixel box.

Table 1. Target properties

Object	Redshift	g_{AB}	r_{AB}	Petro Rad in r (”)	exposure time (min)	Observing date (HST)	M_r
SDSSJ161330.18+510335.5 (E+A)	0.0341±0.0009	15.86	15.38	19.6	50 (core), 60 (north)	July, 29, 2005	-20.5
SDSSJ161332.23+510342.9 (companion)	0.0339±0.001	15.89	15.09	4.6	50 (core), 60 (north)	July, 29, 2005	-20.7

3 OBSERVATION

Observations were carried out on July 29, 2005 with the FOCAS spectrograph (The Faint Object Camera and Spectrograph; Kashikawa et al. 2002) on board the Subaru telescope. We performed a long-slit spectroscopy with the slitwidth of 1.0” on the position A (core) and B (north) of Fig.1. Both slits cover the E+A galaxy and the companion galaxy simultaneously. We used the `VPH350` grism, which provides us with the wavelength coverage of 3800-5250Å, with the resolution of R ~1600. We used 3×1 binning mode, giving the pixel size of 0.311”/pixel in a spatial direction. The seeing was ~1.6” based on a bright star we simultaneously placed on the slit. The exposure time was 600+1200×2 seconds for the slit A (centre), and 1200×3 seconds for the slit B (north). We moved the target along the slit ±2 arcsec between the exposures to remove systematic effects.

The data reduction was performed with the standard procedure with the IRAF; The overscan subtraction, distortion correction, and the flat-fielding were performed. We used a Th-Ar lamp for the wavelength calibration. Then, frames were combined after the spacial shift were accounted for. Background subtraction and the extraction of the spectra are carried out in a standard manner. A standard star HZ44 observed with the 2.0” slit was used for the flux calibration. In Fig.2, we show spectra of the two galaxies obtained from each slit. It is immediately noticed that the E+A galaxy has strong Balmer absorption lines along with an A-star like continuum. The spectra of the companion galaxy are dominated by old stars with deep Ca H&K absorptions. Both galaxies have weak emissions in [OII] and possibly in [OIII], which will be discussed later. Measured redshifts based on [OII], CaH&K lines are 0.0341±0.0009 and 0.0339±0.001 for the E+A and companion, respectively. These values are consistent with the redshift measured by the SDSS (0.034±0.00012) and by Yagi, Goto, & Hattori (2006). The relative velocity is 61.8 km/s. One arcsec corresponds to 0.66 kpc at this redshift.

One of the main purpose of this observation was to carry out spatially-resolved analysis. To this purpose, we have divided the 20.3-25.5 arcsec of aperture into 9 equally spaced bins for each spectrum. And thus, the size of each bin (2.3-2.8”) is larger than the PSF size of 1.6”. In Fig. 3, we show spectrum of each bin for both galaxies.

Using these spectra, we measured equivalent widths of [OII], Hδ, Hγ, Hβ and [OIII] lines using the flux summing technique in Goto et al. (2003c). The wavelength ranges used are presented in Worthey & Ottaviani (1997); Miller & Owen (2002). The strength of the 4000 Å break (D4000) was measured using the definition in Stoughton et al. (2002).

4 RESULTS

4.1 Line flux profile

In Fig.4, we show normalized flux profiles of the measured lines. Profiles are normalized at a peak flux. Fluxes for absorption lines are measured by integrating the amount of absorption under the fitted-continuum, i.e., they are pseudo-flux measured in a similar way to emission line fluxes. The right two panels show the profile for the E+A galaxy. Absorption lines (Hδ,Hγ,and Hβ) connected with the solid lines show a perfect agreement with each other. Interestingly, [OIII] emission line peaks 4 arcsec away from the absorption peak on the bottom-right panel and -4 arcsec away on the top-right panel, possibly indicating that the current star formation is going on at a different location from the post-starburst region. [OII] emission is too noisy to locate the peak of the profile.

For a companion galaxy on the left panels, only Hβ (magenta squares) and [OII] (green filled circles) have enough signal-to-noise to measure profiles. The peaks of these two profiles agree with each other. The [OII] emission shows a slightly extended profile.

4.2 Equivalent widths profile

In Fig.5, we present EW distribution of three absorption lines (Hδ,Hγ,and Hβ) and two emission lines ([OII] and [OIII]) for the E+A/companion galaxies in the core/north spectra. The right panels show EWs for the E+A galaxy. The bottom panel is from the core, the top panel is from the north spectra. The symbols are the same as the Fig.4. Unlike the flux profile (Fig.4), EWs are not affected by the luminosity profile of the galaxy, and thus, suitable to trace the efficiency in producing emission/absorption. In the right panel of Fig.5, all the absorption lines have very large EW galaxy wide; Hδ (red diamonds) EW is > 7Å galaxy wide in both core/north spectra ($>$13 arcsec wide or $>$8.5 kpc). There is no significant radial trend for Hδ. Hγ (orange triangles) and Hβ (magenta squares)EWs stay at $\sim$6 and 4 Å, respectively, for the entire galaxy except for the low S/N regions at the edge. Emission lines have very weak EWs: [OIII] EWs are 1Å or less for everywhere; [OII] EWs are also small. Although in Fig. 3, we see a spectrum with emission lines, these emission lines are weak as in Fig.5. Therefore, we can still call this galaxy as an E+A galaxy.

For a companion galaxy, spectra are shown in the left panels of Fig.3. The bottom-left panel is for the core spectrum, the top-left panel is for the north spectrum. For this companion galaxy, Hδ and Hγ absorption lines are weak, indicating the stellar population is old. The only line securely detected is Hβ, which has a flat profile with $\sim$2Å of EWs. There is no significant radial trend. [OII] line is detected with 4-5Å around the galaxy centre. The [OII] emission is stronger for the companion than for the E+A.

4.3 Rotation

With the resolution of $R \sim 1600$, we have a chance to measure rotational velocity of galaxies. We fit a Gaussian to the Hδ (absorption) line, to measure the red/blue shifted central wavelength. In other occasions, emission lines such as [OII] or [OIII] are preferred for this exercise. In our particular case, however, the Hδ (absorption) line is much stronger than the emission lines, providing us with a better measurement of the rotation curve.We visually inspected the goodness of the Gaussian fit and only spectra where the line has sufficient signal-to-noise ratio are used.

In Fig.6, we show the recession velocity from the Hδ line. In the right panel, the diamonds (blue) and triangles (green) are for the core/north E+A spectra. There may be a slight sign of the rotation of $\sim$50km/s in the core spectra (blue diamonds). However, this is below the resolution of the spectra, and the trend can not be recognized in the north spectra (green triangles). Therefore, we do not claim a rotation of the core/north E+A spectra.

The squares (magenta) and crosses (red) in the left panel of Fig.6 are for the companion galaxy in the core/north. A clear rotation curve is found from the position of the $X = -6$ arcsec to $X = +3$ arcsec. The rotation observed for the companion galaxy is greater than 175 km/s.

It is interesting to find no significant rotation for a galaxy that has just experienced a starburst (E+A). This suggests following possibilities: (i) the galaxy-galaxy dynamical interaction destroyed the rotation of the galaxy (however the companion galaxy has the rotation); (ii) the progenitor of the E+A galaxy was not a rotationally-supported disk galaxy, although it possessed enough gas to create a starburst; or (iii) the rotation of the E+A galaxy is face-on although we do not see an obvious face-on disk in Fig.1.

It is also puzzling that the companion galaxy whose spectra look like that of an elliptical galaxy has rotational velocity. One possibility is that the rotational velocity originates from the dynamical interaction, although no rotation was found for the E+A galaxy. Another possibility is that in Fig.1, the core of the companion galaxy is slightly extended toward the north-east direction, implying a possible position-angle of the former disk component. Thus, the companion galaxy may have been a rotationally-supported disk galaxy before the dynamical interaction started.

We also tried to measure the velocity dispersion for both the E+A and the companion galaxies. Our method is similar to that utilized by the SDSS spectroscopic pipeline; first we masked out possible emission lines, then the rest of the spectra are fit with the combination of eigen spectra with varying velocity dispersion. The measured velocity dispersions are 279±49, 224±31 km/s for the E+A and companion galaxies, respectively. The results suggest that galaxies have comparable mass, and thus, the system is experiencing an equal-mass (major) merger with the mass ratio close to 1. The derived mass ratio is consistent with Bekki, Shioya, & Couch (2001)’s prediction that requires mass ratio of > 0.3 to create an E+A galaxy.

4.4 Metallicity estimate

Next, we would like to estimate age and burst strength (stellar mass ratio of young population to old stellar population) of these two galaxies by comparing observational data with models. To do this, however, we first need to estimate metallicity of these galaxies since there is a well-known fact that galaxy age and metallicity are degenerated in optical colour or spectra. This age-metallicity degeneracy can be lifted when you have near-infrared photome-

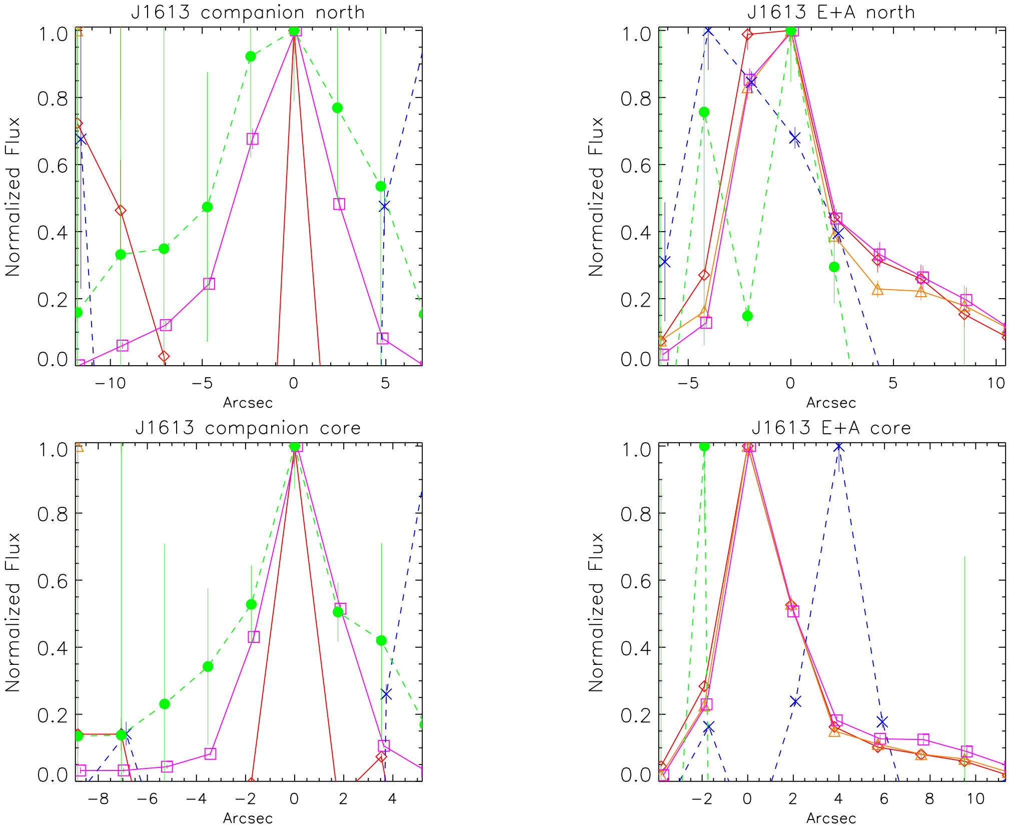

Figure 4. Normalized flux profiles: The right panels show the normalized flux profiles for the E+A core (lower) and north (upper) spectra. The left panels show the normalized flux profiles for the companion core (lower) and north (upper) spectra. The diamond (red), triangle (orange), and square (pink) symbols are for Hδ, Hγ and Hβ, respectively. These absorption lines are connected with the solid lines. The cross (blue) and filled (green) circle are for [OIII] and [OII] emission lines, which have positive sign in this plot. The emission lines are connected with the dotted lines. The abscissa is shifted so that the Hδ flux peaks at $X=0$. One arcsec corresponds to 0.66 kpc at this redshift.

try in hand; optical-near-infrared colour such as $V-K$ is a measure of the temperature of its red giant branch. The temperature is strongly dependent on metallicity but has little sensitivity to age (Puzia et al. 2002; Brodie & Strader 2006; Cantiello & Blakeslee 2007). In Fig.7, we plot $r-H$ colour against $r-i$ colour. Optical colours are from the SDSS. The H-band image was taken with the SQUIID NIR camera on board the KPNO2m telescope on the night of June 4th, 2006. A complete analysis of these data will be presented elsewhere. The seeing sizes were similar among r, i and H-bands. Fluxes are measured in a fixed aperture of 3" at the centre.

In Fig.7, Overplotted lines are the SED models; We constructed model SEDs with GALAXEV (Bruzual & Charlot 2003, hereafter BC03), using the extinction law by Cardelli, Clayton, & Mathis (1989), and Salpeter IMF. Metallicities are changed in the range of $0.0004 \leqslant Z \leqslant 0.02$. The model galaxies evolve for 10Gyr with an exponentially decreasing star-formation rate (τ=1 Gyr), and then a secondary instantaneous burst occurs; The dots represent 100, 200, 300, 500 Myrs and 1Gyr of time after the instantaneous burst.

This $(r-i)$ vs $(r-H)$ diagram is advantageous in determining the metallicity of galaxies when a spectrum does not cover Fe or Mg lines. Three colours (r, i, H) are carefully chosen so that age, burst-strength, and dust-extinction are degenerate in one (straight) direction perpendicular to the metallicity variation. Only possible alternative is $r-z-K_s$ colour among general broad-band optical-NIR filters. In other choices of colours, the models curve and overlaps with each other. In fact in Fig.7, age vectors (lower-left to upper-right in the Figure) are almost perpendicular to the metallicity change. The models with different burst-strengths (we checked 50, 30, 10, 5, 3 and 1%) are almost overlapped with each other, i.e., no degeneracy with the metallicity. Moreover, the dust reddening vector (shown with an arrow in the Figure) is almost parallel to the aging vector in this diagram. Therefore, the $(r-i)$ vs $(r-H)$ diagram provides us with a useful tool to measure metallicity of nearby poststarburst galaxies whose young population is 100M-1Gyr.

Measured colours of the E+A galaxy and the companion galaxy are shown with the black dots in Fig.7. The E+A and companion galaxies are better described with the metallicity of $Z=0.008$ (i.e., 0.4×solar metallicity) and $Z=0.02$, respectively. We will assume $Z=0.008$ in the next section to estimate the E+A's age.

In this paper, these colour based metallicity measurements are merely meant to aid the age determination in the following section. A more careful treatment such as high S/N spectroscopy covering Fe and Mg lines is needed if one wishes to obtain physical implications based on the metallicity measurement.

4.5 Age estimate

In Fig.8, we plot Hδ EW against the strength of the 4000Å break (D4000). This diagram has been used as a good tool to estimate

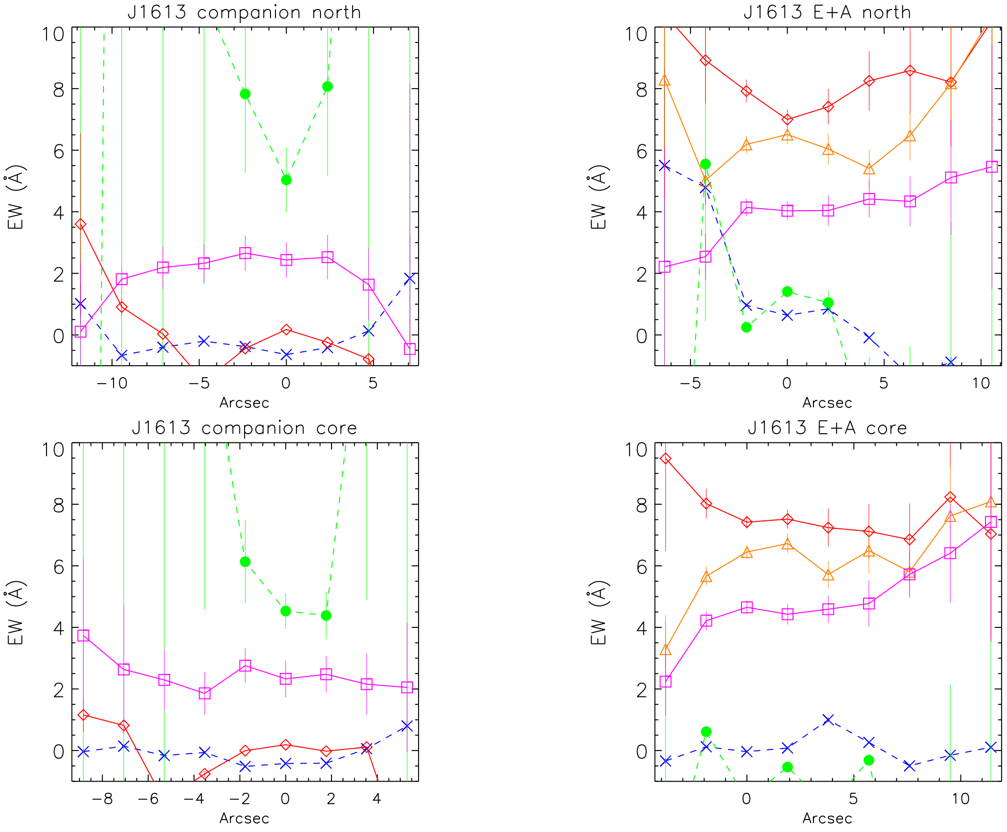

Figure 5. Equivalent width (EW) profiles: The right panels show the EW profiles for the E+A core (lower) and north (upper) spectra. The left panels show the EW profiles for the companion core (lower) and north (upper) spectra. The diamond (red), triangle (orange), and square (magenta) symbols are for Hδ, Hγ and Hβ, respectively. These absorption lines are connected with the solid lines. The cross (blue) and filled (green) circle are for [OIII] and [OII] emission lines, which have positive sign in this plot. The emission lines are connected with the dotted lines. One arcsec corresponds to 0.66 kpc at this redshift.

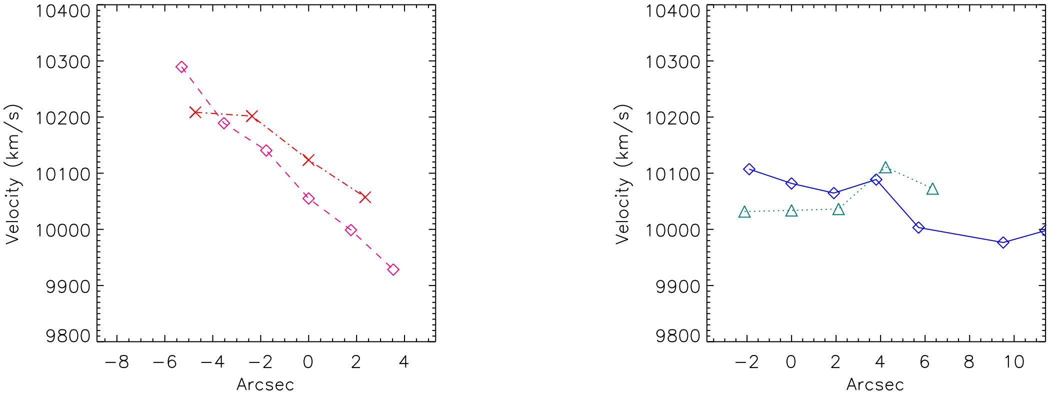

Figure 6. Recession Velocity. We plot recession velocity of the Hδ line. The diamonds and triangles in the right panel are for the E+A core/north spectra, respectively. The squares and crosses are for the companion galaxy's core/north spectra in the left panel. We visually checked the gaussian fits, and only data points based on a reasonably good fit are shown. One arcsec corresponds to 0.66 kpc at this redshift.

age, stellar-mass, and star-formation-history of galaxies (e.g., Goto 2003; Kauffmann et al. 2003; Yagi, Goto, & Hattori 2006). Symbols for data points are the same as in Fig.6. We overplot population synthesis models of Bruzual & Charlot (2003) with Salpeter IMF and metallicity of $Z = 0.008$ (See Section 4.4). We have checked that a small change in metallicity $Z = 0.008 - 0.02$ does not affect the discussion below. Over the 10-Gyr-old stellar population with an exponentially-decaying star formation rate (τ=1Gyr), we added 5,10, and 50% (in terms of stellar mass) of instantaneous starburst population. The 100% burst in the Figure is a pure burst with no underlying old stellar population. In each model, we marked 0.1, 0.25, 0.5, and 2 Gyrs of ages (after the instantaneous

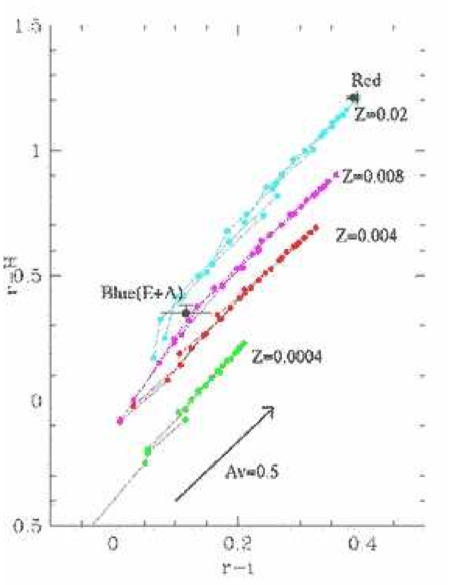

Figure 7. The $r-i$ vs $r-H$ colour-colour diagram. The solid lines with small dots are models based on Bruzual & Charlot (2003) at z=0.034 with varying metalicity. Colours of E+A and companion galaxy are shown with filld circles.

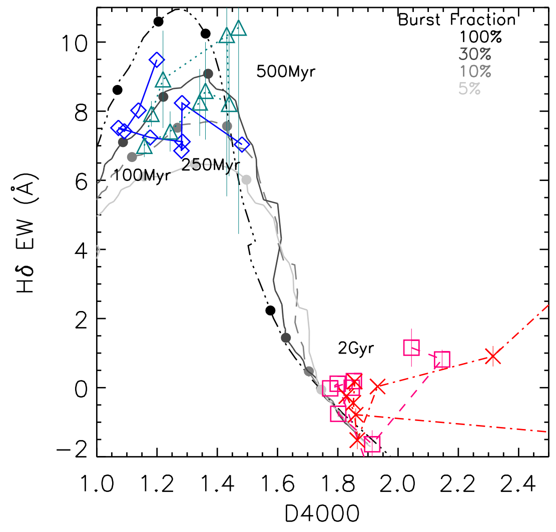

Figure 8. Hδ EW is plotted against D4000. The diamonds and triangles are for the E+A core/north spectra, respectively. The squares and crosses are for the companion galaxy's core/north spectra. Gray lines are population synthesis models from Bruzual & Charlot (2003) with 5-100% delta burst population added to the 10G-year-old exponentially-decaying (τ=1Gyr) underlying stellar population. Salpeter IMF and metallicity of $Z = 0.008$ (See Section 4.4) are assumed. On the models, burst ages of 0.1, 0.25, 0.5 and 2 Gyr are marked with the filled circles. See Yagi, Goto, & Hattori (2006) for more details of the models.

starburst) with the filled circles. These are the same models used in Yagi, Goto, & Hattori (2006).

By comparing models with data, E+A galaxies are most consistent with the 30% burst model with the age of 250 Myr although the burst strengths of 5-30% with the age of 100-500 Myrs are allowed within the error. It seems that the core of the E+A galaxy has slightly yonger age (∼100 Myr) than outskirts (∼500 Myr). This trend is more consistent with the age difference than the difference in burst fraction, suggesting the galaxy core had experienced starburst more recently. One end facing to the companion seems to have a larger burst fraction ($> 30\%$) than the other end (10%). In any case, the comparison suggests that the E+A galaxy is in its very young phase (∼250 Myr) of the post-starburst. On the other hand, the companion galaxy is consistent with much larger age of >2 Gyr. Although the companion galaxy has a weak [OII] emission, this indicates that major star formation activity of the companion galaxy ceased well-in-advance to the current galaxy merger/interaction.

In Fig.9, we compare [OII] EWs and Hδ EWs. Symbols are the same as in previous figure. Overplotted models are from Bekki, Shioya, & Couch (2001). Their dusty-starburst and dust-free merger models of equal mass are with filled-circles and asterisks, respectively. We marked the ages (after the burst) of 40Myr-1.5Gyrs. The E+A galaxy is consistent with ∼400 Myr of age of the dusty-starburst model after the starburst. The data points of the companion galaxies (magenta squares and red crosses) deviate from the models, and cannot be explained within the model assumption of an equal mass merger of gas rich disks. Perhaps, the J1613+5103 is a wet-dry merger system, where the dry galaxy (companion) had a little remaining gas to induce star formation.

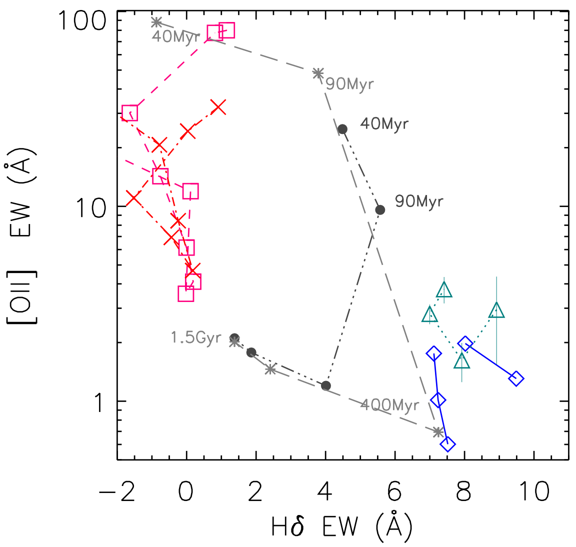

Figure 9. Hδ EW is plotted against [OII] EW. The diamonds and triangles are for the E+A core/north spectra, respectively. The squares and crosses are for the companion galaxy's core/north spectra. Only data points with positive [OII] EW (i.e., in emission) are used. Gray lines are major-merger models from Bekki, Shioya, & Couch (2001) with the ages (after the burst) of 40Myr-1.5Gyrs. Asterisks and filled-circles are for dust-free and dusty-starburst models, respectively.

5 DISCUSSION

5.1 Comparison to previous work

In this subsection, we summarize previous work on spatially-resolved spectroscopy of E+A galaxies, and compare them to our results.

Caldwell et al. (1996) obtained long-slit spectra of E+A galaxies in the Coma cluster and showed that starburst signatures are prominent in the central core and are spatially extended. Similarly, Norton et al. (2001) found that the young stellar populations are more centrally concentrated than the older populations, but they are not confined to the galaxy core (radius $<$1 kpc). Recently, Yagi & Goto (2006) performed spatially-resolved spectroscopy of three E+A galaxies using the APO3.5m telescope. They found that the post-starburst region is as extended as the old population with no significant age gradient along the radius, concluding that the post-starburst in the E+As is a galaxy-wide phenomenon. Swinbank et al. (2005) observed a Hδ-strong galaxy with a weak [OII] emission from the Goto et al. (2003c) catalogue, and found that A-type stars are widely distributed across the system and are not centrally concentrated. Note, however, that this galaxy had a weak emission in [OII] (4.1Å), and thus, cannot be called as an E+A galaxy in our definition.

It is important to keep in mind that these work has each own biases in sample selections, observations and analysis methods. Especially, earlier samples often lacked information on Hα, resulting in inviting contamination from Hα emitting galaxies up to 52% (See Goto et al. 2003c). Majority of the above work, however, concluded that the post-starburst phenomena was centrally-concentrated in most cases, and significantly extended to a few kpc, being consistent with a theoretical prediction for merger/interaction remnant. These results were unique in that without using information on the global/external properties of E+A galaxies, but yet reached a similar conclusion on the origin of E+A galaxies. For example, Goto (2005) found an excess in the number of companion galaxies of E+A galaxies, concluding that it is an evidence of the merger-interaction. Many authors reported disturbed morphologies of E+A galaxies point to the merger/interaction origin (Oegerle, Hill, & Hoessel 1991; Blake et al. 2004; Liu et al. 2007).

However, our results may create a stir on the interpreation of the previous work; the E+A system J1613+5103 is cleary a dynamically-interacting system. In Yagi, Goto, & Hattori (2006), we reported a flat, uniform Hδ distribution of 5 kpc. In this work, we confirmed the result with deeper and more extended observation, and found that the post-starburst feature is extended to 8.5 kpc, instead of the centrally-concentrated post-starburst region which was expected based on the merger-interaction scenario of the E+A origin. We discuss possible implication of our results in the next subsection.

The colour gradient of this E+A galaxy was studied in detail by Yamauchi & Goto (2005), who found that the $g-r$ and $r-i$ colours are bluer in the central region within 1.9 kpc (see their Fig.3, galaxy #1). While we found a flat distribution of Hδ EWs in the right panels of Fig.5, their result again implies the existence of the age gradient; looking at the models in Fig.8, Hδ EW does not evolve much in the first 500Myrs, especially when the burst fraction is low. In this period of $<$500Mrs, however, the D4000, which is equivalent to the colour measured out of spectra, keeps becoming larger (redder). For clarity, we plot the radial profile of the D4000 in Fig.10, where the right panel is for the E+A core/north spectra and the left panels are for the core/north spectra of the companion. In the right panel, the D4000 is smaller with smaller than 1.2 at around $-2<X<4$ arcsec, which corresponds to 4 kpc wide area around the centre, in good agreement with the colour gradient of Yamauchi & Goto (2005).

5.2 Physical interpretation

In this series of papers (Yagi, Goto, & Hattori 2006, and this work) we have found the following: Our target E+A galaxy, J1613+5103, has a companion galaxy 14 kpc away with the velocity difference of 61.8 km/s. Both the E+A and companion galaxies have disturbed morphology with the core and a fan-shaped region extended away from each other. With these evidences, there is little doubt that the system is dynamically interacting galaxies. Age estimate based on the Hδ-D4000 (Fig.8) or Hδ-[OII] (Fig.9) diagrams suggest $\sim$250 Myr after the burst, being consistent with the early stage of a dynamical interaction. In addition, the existence of such system presents an important example that a dynamical galaxy-galaxy interaction can create an E+A galaxy as a matter of fact, and that the companion galaxy of the E+A system does not have to be an E+A galaxy.

In Section 4, we found that Hδ EW of the E+A galaxy is very strong with $>$7Å in the entire galaxy with no obvious spatial trend, despite the fact that the galaxies are dynamically interacting. The results are inconsistent with the previously believed simplified picture: during a galaxy-galaxy interaction, the gas readily loses angular momentum due to dynamical friction, decouples from the stars, and inflows rapidly toward the merger nuclei (Barnes 1992; Barnes & Hernquist 1992, 1996; Mihos & Hernquist 1994, 1996), creating a central starburst, which could evolve into E+A phase if the truncation of the starburst is rapid enough (Goto 2004). In this scenario, the galaxy is left with a central population of young stars and hence a radial distribution of Hδ EW which is the highest in the centre and decreases rapidly with galactocentric radius (Pracy et al. 2005; Bekki et al. 2005).

This scenario was the basis of the spatially-resolved observational work in the literature; Yagi & Goto (2006); Goto et al. (2008) found centrally-concentrated post-starburst regions (but significantly extended) in E+A galaxies, concluding it is an evidence of merger origin of the E+A galaxies. On the contrary, if the stripping is the cause of the E+A phenomena, the star-formation is simultaneously and uniformly truncated throughout the entire disc, creating a flat, uniformly high $H\delta$ EW profile (Pracy et al. 2005).

However, our results present an example where dynamical interaction also can create a flat, uniform radial distribution of the post-starburst region. The discovery complicates the picture; investigating a spatial distribution of the post-starburst region may not be a good way to investigate the origin of the E+A phenomena. In the case of J1613+5103, an obvious companion is present, and thus, it is easy to be judged as an interaction. However, if the minor-merger can also create such a flat profile, there is no way to distinguish from the stripping scenario. Our example cautions us that it is important to combine multiple informations together to investigate the physical origin of E+A galaxies.

We also found that this system is likely to be an equal mass merger based on the velocity dispersion. The result is consistent with Bekki et al. (2005) which predicted at least a mass ratio of 0.3 is required to create an E+A galaxy through dynamical galaxy merger simulation. It is important to measure the mass of more E+A companion galaxies to constrain the mass ratio required to create an E+A galaxy. An attempt to spectroscopically follow-up E+A companions is on-going (Yamauchi, Yagi & Goto 2008).

It is interesting that we found rotational velocity only in the

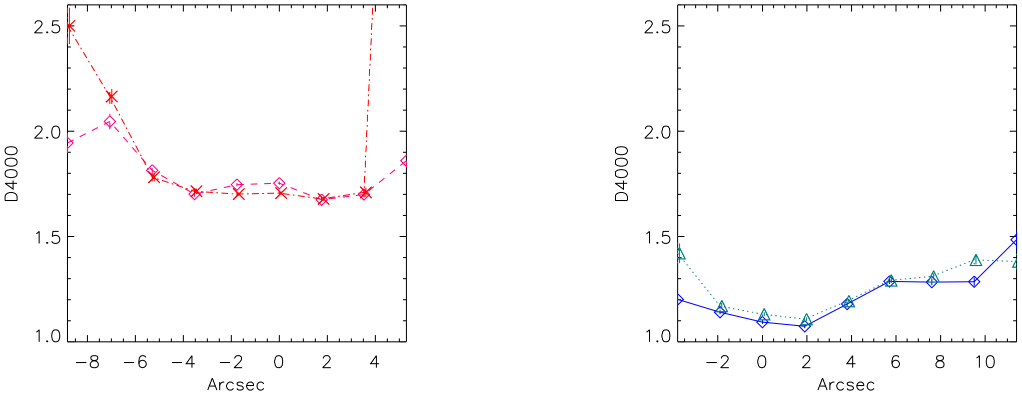

Figure 10. The radial profile of the 4000Åbreak (D4000). The diamonds and triangles in the right panel are for the E+A core/north spectra, respectively. The squares and crosses are for the companion galaxy's core/north spectra in the left panel. One arcsec corresponds to 0.66 kpc at this redshift.

companion galaxy (Fig.6), which did not experience a starburst. This velocity could be provoked by the dynamical interaction of the two galaxies. However, considering that these two galaxies have similar mass, and the other (E+A) does not have rotational velocity, it is more plausible that the progenitor of the companion galaxy was a rotationally supported disk galaxy. There is a hint of disk plane in Fig.1. Considering that the companion galaxy did not have major star-formation at least for recent 2 gigayears (Fig.8), the progenitor of the companion galaxy may have been a passive, rotationally-supported S0 galaxy. It also means that for at least 2 gigayears, galaxy can sustain the rotational velocity without continuing star formation activity.

But then, why E+A galaxy do not show rotational velocity even though it has experienced the starburst? We have to keep in mind that the E+A could be face-on although we do not see an obvious face-on disk in Fig.1. Since the rotational velocity of the companion galaxy is not destroyed by the dynamical interaction, it is not likely that the E+A galaxy had an initial rotation. But at the same time, E+A galaxies had experienced a starburst, therefore, must have had significant amount of gas, and possibly some star-formation activity even before the starburst. Taken all these together, one possibility, assuming not face-on, is that the progenitor of E+A galaxy in case of J1613+5103 may have been a pressure-supported, star-forming elliptical galaxy, which is quite rare in the present Universe.

We found a weak emission in [OII] and [OIII] for both the E+A and companion galaxies. The finding of the [OII] emission line is apparently inconsistent with our selection criteria of E+A galaxies with no significant [OII] nor Hα emission ([OII] EW $< 2.5\AA$ and Hα EW $< 3.0\AA$). However, the detected emission is weak with EW$\sim$1Å for both [OII] and [OIII]. Using the prescription for the [OII] line given in Hopkins et al. (2003), the star formation rate of this galaxy is 0.06$M_{\odot}yr^{-1}$, which is small enough to be negligible compared with the post-starburst population. Our spectra have higher resolution of $R\sim$1600 than those of the SDSS and Yagi, Goto, & Hattori (2006). When we smooth the spectra to the resolution of the SDSS, the emission lines become almost invisible. This is perhaps why previous spectra did not detect the emission, and due to the same reason, we still regard the galaxy as an E+A galaxy in the post-starburst phase.

The location of the emission lines in the E+A galaxy is puzzling. The [OII] emission lines do not have enough signal-to-noise ratio to probe the location. But the [OIII] emission, at the core spectrum (the upper left panel of Fig.4), the [OIII] emission peaks at +4 arcsec away from the peak of the absorption line. The location is almost outside of the core region, and around the border of the fan-shaped extended region in Fig.1. However, in the north spectra (the upper right panel of Fig.4), the [OIII] emission is peaked at the -4 arcsec, right in front of the companion galaxy. These locations suggest that [OIII] emission may come from outside of the post-starburst (strong Balmer absorption) core. However, the presence of only a single peak at both the core and north spectra at an opposite direction suggests that the [OIII] emission does not form a symmetric ring/sphere star-forming region, but instead it has more complicated spatial distribution. In this context, it will be very interesting to perform an IFU spectroscopy such as in Swinbank et al. (2005); Goto et al. (2008) for this E+A system. In the literature, Swinbank et al. (2005) observed a Hδ strong galaxy SDSSJ101345.39+011613.66 (Goto et al. 2003c) with the Gemini IFU, and found a similar offset of [OII] emission line from the Balmer absorptions by $\sim$2 kpc.

For the companion galaxy, only the [OII] emission has a good enough signal-to-noise ratio to probe the spatial distribution (bottom panels of Fig.4). The peak location of [OII] agrees with that of Balmer absorption lines, but the emission is slightly more extended to ±5 arcsec on both sides, suggesting that the [OII] emission plausibly triggered by the interaction is widely distributed beyond the core region. The overall spectra of the companion galaxy are dominated by the old stellar population (Fig.3), and thus, it is not likely that the companion galaxy is experiencing a strong starburst of more than 5% (Yagi & Goto 2006). Perhaps, a small amount of gas remaining in the companion galaxy was disturbed by the interaction to create a weak [OII] emission observed here. Since the emission is spatially extended, the origin of the [OII] is not likely a central AGN. The weak [OIII] emission at the centre also supports the lack of AGN.

6 CONCLUSIONS

We have performed a spatially-resolved long-slit spectroscopy of the nearby interacting E+A system J1613+5103 using the FOCAS/Subaru. The E+A galaxy with very strong Hδ EW of $\sim$7Å (estimated age of 250Myr) has an obvious companion at 14 kpc in front. Combined with a disturbed morphology, the system is a clear example that a dynamical interaction can actually create an E+A galaxy. The slit was aligned to include cores of both the E+A galaxy and the companion galaxy. Additional spectra were taken at 2 arcsec away in the north from the cores. Our finding based on these spectra are as follows:

- The strong Balmer absorption lines of the E+A galaxy are strong in the entire galaxy; Especially, Hδ EW is $>$7Å for the entire galaxy region ($>$8.5 kpc).
- The peak of the weak (EW$\sim$1Å) [OIII] emission of the E+A galaxy is slightly offset from that of the Balmer absorption lines, possibly suggesting that the remaining starburst is going on at a different location from the post-starburst region.
- For the companion galaxy emission line ([OII]) profile is more extended than that of the Hβ, suggesting on-going star-formation happens in more extended region than the central region of old stellar population.
- We found a rotational velocity of $>$175 km/s for the companion galaxy (Fig.6), implying the companion was a disk galaxy without star-formation activity before the dynamical interaction. No significant rotation was found for the E+A galaxy.
- Using the $r-H$ colour, we estimated the metallicity of the E+A and the companion were $Z=0.008$ and 0.02, respectively (Fig.7).
- Based on the Hδ-D4000 and Hδ-[OII] EW plots (Fig.8), we estimate age of the E+A galaxy is around 250 Myr after the truncation of the burst. Possibly the centre of the E+A has a slightly younger age of $\sim$100 Myr than its outskirts.

These results present an important example that a galaxy-galaxy interaction with equal mass can create a galaxy wide, uniformly-distributed post-starburst regions. In this example, it is obvious that the dynamical interaction is the physical origin of the E+A galaxy. At the same time, it warns us that simple classification of the E+A origin with the Hδ profile may not be adequate enough.

ACKNOWLEDGMENTS

We thank the anonymous referee for many insightful comments, which significantly improved the paper. We are grateful to T.Hattori for valuable help during the observation. We thank Youichi Ohyama for useful discussions.

T.G. acknowledges financial support from the Japan Society for the Promotion of Science (JSPS) through JSPS Research Fellowships for Young Scientists.

The research was financially supported by the Sasakawa Scientific Research Grant from The Japan Science Society. This research was partially supported by the Japan Society for the Promotion of Science through Grant-in-Aid for Scientific Research 18840047.

The authors wish to recognize and acknowledge the very significant cultural role and reverence that the summit of Mauna Kea has always had within the indigenous Hawaiian community. We are most fortunate to have the opportunity to conduct observations from this sacred mountain.

Funding for the creation and distribution of the SDSS Archive has been provided by the Alfred P. Sloan Foundation, the Participating Institutions, the National Aeronautics and Space Administration, the National Science Foundation, the U.S. Department of Energy, the Japanese Monbukagakusho, and the Max Planck Society. The SDSS Web site is http://www.sdss.org/.

The SDSS is managed by the Astrophysical Research Consortium (ARC) for the Participating Institutions. The Participating Institutions are The University of Chicago, Fermilab, the Institute for Advanced Study, the Japan Participation Group, The Johns Hopkins University, Los Alamos National Laboratory, the Max-Planck-Institute for Astronomy (MPIA), the Max-Planck-Institute for Astrophysics (MPA), New Mexico State University, University of Pittsburgh, Princeton University, the United States Naval Observatory, and the University of Washington.

REFERENCES

Abadi M. G., Moore B., Bower R. G., 1999, MNRAS, 308, 947
Abraham R. G., et al., 1996, ApJ, 471, 694
Adelman-McCarthy J. K., et al., 2006, ApJS, 162, 38
Barger A. J., Aragon-Salamanca A., Ellis R. S., Couch W. J., Smail I., Sharples R. M., 1996, MNRAS, 279, 1
Barnes J. E., 1992, ApJ, 393, 484
Barnes J. E., Hernquist L., 1992, ARA&A, 30, 705
Barnes J. E., Hernquist L., 1996, ApJ, 471, 115
Bekki K., Couch W. J., Shioya Y., Vazdekis A., 2005, MNRAS, 359, 949
Bekki K., Couch W. J., 2003, ApJ, 596, L13
Bekki K., Couch W. J., Shioya Y., 2002, ApJ, 577, 651
Bekki K., Shioya Y., Couch W. J., 2001, ApJ, 547, L17
Bekki K., Shioya Y., 1998, ApJ, 497, 108
Belloni P., Bruzual A. G., Thimm G. J., Roser H.-J., 1995, A&A, 297, 61
Blake C., et al., 2004, MNRAS, 355, 713
Blanton M. R., et al., 2003, ApJ, 594, 186
Blanton M. R., et al., 2003, ApJ, 592, 819
Cantiello M., Blakeslee J. P., 2007, ApJ, 669, 982
Broadhurst T. J., Ellis R. S., Shanks T., 1988, MNRAS, 235, 827
Brodie J. P., Strader J., 2006, ARA&A, 44, 193
Bruzual G., Charlot S., 2003, MNRAS, 344, 1000
Butcher H., Oemler A., Jr., 1978, ApJ, 226, 559
Caldwell N., Rose J. A., Franx M., Leonardi A. J., 1996, AJ, 111, 78
Cardelli J. A., Clayton G. C., Mathis J. S., 1989, ApJ, 345, 245
Couch W. J., Barger A. J., Smail I., Ellis R. S., Sharples R. M., 1998, ApJ, 497, 188
Couch W. J., Sharples R. M., 1987, MNRAS, 229, 423
Dressler A., Oemler A. J., Poggianti B. M., Smail I., Trager S., Shectman S. A., Couch W. J., Ellis R. S., 2004, ApJ, 617, 867
Dressler A., Smail I., Poggianti B. M., Butcher H., Couch W. J., Ellis R. S., Oemler A. J., 1999, ApJS, 122, 51
Dressler A., Gunn J. E., 1992, ApJS, 78, 1
Dressler A., Gunn J. E., 1983, ApJ, 270, 7
Fisher D., Fabricant D., Franx M., van Dokkum P., 1998, ApJ, 498, 195
Fabricant D. G., McClintock J. E., Bautz M. W., 1991, ApJ, 381, 33
Farouki R., Shapiro S. L., 1980, ApJ, 241, 928
Filippenko A. V., 1982, PASP, 94, 715
Fujita Y., Takizawa M., Nagashima M., Enoki M., 1999, PASJ, 51, L1
Fujita Y., Takizawa M., Sarazin C. L., 2003, ApJ, 584, 190
Fujita Y., Goto T., 2004, PASJ, 56, 621
Fukugita M., Shimasaku K., Ichikawa T., 1995, PASP, 107, 945
González Delgado R. M., Leitherer C., Heckman T. M., 1999, ApJS, 125, 489

Goto T., Kawai A., Shimono A., Sugai H., Yagi M., Hattori T., 2008, MNRAS, 386, 1355
Goto T., 2007b, MNRAS, 381, 187
Goto T., 2007a, MNRAS, 377, 1222
Goto T., 2005, MNRAS, 357, 937
Goto T., 2004, A&A, 427, 125
Goto T., Yamauchi C., Fujita Y., Okamura S., Sekiguchi M., Smail I., Bernardi M., Gomez P. L., 2003d, MNRAS, 346, 601
Goto T., et al., 2003a, PASJ, 55, 739
Goto T., et al., 2003b, PASJ, 55, 757
Goto T., et al., 2003c, PASJ, 55, 771
Goto T., 2003, PhD. Thesis, The University of Tokyo
Gunn J. E., Gott J. R. I., 1972, ApJ, 176, 1
Hopkins A. M., et al., 2003, ApJ, 599, 971
Hubble E. P., 1926, ApJ, 64, 321
Kashikawa N., et al., 2002, PASJ, 54, 819
Kauffmann G., et al., 2003, MNRAS, 341, 33
Kent S. M., 1981, ApJ, 245, 805
Komatsu E., et al., 2008, arXiv, 803, arXiv:0803.0547
Lavery R. J., Henry J. P., 1986, ApJ, 304, L5
Liu C. T., Hooper E. J., O'Neil K., Thompson D., Wolf M., Lisker T., 2007, ApJ, 658, 249L
MacLaren I., Ellis R. S., Couch W. J., 1988, MNRAS, 230, 249
Mihos J. C., Hernquist L., 1996, ApJ, 464, 641
Mihos J. C., Hernquist L., 1994, ApJ, 425, L13
Miller N. A., Owen F. N., 2002, AJ, 124, 2453
Morris S. L., Hutchings J. B., Carlberg R. G., Yee H. K. C., Ellingson E., Balogh M. L., Abraham R. G., Smecker-Hane T. A., 1998, ApJ, 507, 84
Newberry M. V., Boroson T. A., Kirshner R. P., 1990, ApJ, 350, 585
Norton S. A., Gebhardt K., Zabludoff A. I., Zaritsky D., 2001, ApJ, 557, 1
Oegerle W. R., Hill J. M., Hoessel J. G., 1991, ApJ, 381, L9
Poggianti B. M., Smail I., Dressler A., Couch W. J., Barger A. J., Butcher H., Ellis R. S., Oemler A. J., 1999, ApJ, 518, 576
Pracy M. B., Couch W. J., Blake C., Bekki K., Harrison C., Colless M., Kuntschner H., de Propris R., 2005, MNRAS, 359, 1421
Puzia T. H., Zepf S. E., Kissler-Patig M., Hilker M., Minniti D., Goudfrooij P., 2002, A&A, 391, 453
Quilis V., Moore B., Bower R., 2000, Sci, 288, 1617
Quintero A. D., et al., 2004, ApJ, 602, 190
Roberts M. S., Haynes M. P., 1994, ARA&A, 32, 115
Sharples R. M., Ellis R. S., Couch W. J., Gray P. M., 1985, MNRAS, 212, 687
Spitzer L. J., Baade W., 1951, ApJ, 113, 413
Stoughton C., et al., 2002, AJ, 123, 485
Sugai H., Kawai A., Shimono A., Hattori T., Kosugi G., Kashikawa N., Inoue K. T., Chiba M., 2007, ApJ, 660, 1016
Sugai H., Kawai A., Hattori T., Ozaki S., Kosugi G., Shimono A., Okita Y., 2006, NewAR, 50, 358
Sugai H., et al., 2004, SPIE, 5492, 651
Swinbank A. M., Balogh M. L., Bower R. G., Hau G. K. T., Allington-Smith J. R., Nichol R. C., Miller C. J., 2005, ApJ, 622, 260
Tran K.-V. H., Franx M., Illingworth G. D., van Dokkum P., Kelson D. D., Magee D., 2004, ApJ, 609, 683
Tran K.-V. H., Franx M., Illingworth G., Kelson D. D., van Dokkum P., 2003, ApJ, 599, 865
Worthey G., Ottaviani D. L., 1997, ApJS, 111, 377
Yagi M., Goto T., Hattori T., 2006, ApJ, 642, 152
Yagi M., Goto T., 2006, AJ, 131, 2050
Yamauchi C., Yagi M, Goto T., 2008, MNRAS, in press
Yamauchi C., Goto T., 2005, MNRAS, 359, 1557
Yamauchi C., Goto T., 2004, MNRAS, 352, 815